Catalytic Mechanism of *S*-Ribosylhomocysteinase (LuxS): Stereochemical Course and Kinetic Isotope Effect of Proton Transfer Reactions[†,‡]

Jinge Zhu, Reena Patel, and Dehua Pei*

Department of Chemistry and Ohio State Biochemistry Program, The Ohio State University, 100 West 18th Avenue, Columbus, Ohio 43210

Received May 3, 2004; Revised Manuscript Received June 8, 2004

ABSTRACT: *S*-Ribosylhomocysteinase (LuxS) catalyzes the cleavage of the thioether bond in *S*-ribosylhomocysteine (SRH) to produce homocysteine and 4,5-dihydroxy-2,3-pentanedione (DPD), the precursor of type II bacterial quorum sensing molecule. The proposed mechanism involves a series of proton-transfer reactions, which are catalyzed by an Fe^{2+} ion and two general acids/bases in the LuxS active site, resulting in the migration of the ribose carbonyl group from its C1 to C3 position. Subsequent β-elimination at C4 and C5 positions completes the catalytic cycle. In this work, the regiochemistry and stereochemical course of the proton transfer reactions were determined by carrying out the reactions using various specifically deuterium-labeled SRH as substrate and analyzing the reaction products by ^{1}H NMR spectroscopy and mass spectrometry. Our data indicate a suprafacial transfer of the ribose C2 proton to its C1 position and the C3 proton to the C2 position during catalysis, whereas the ribose C4 proton is completely washed into solvent. The primary deuterium kinetic isotope effect suggests that the conversion of 2-keto intermediate to 3-keto intermediate is partially rate limiting. However, mutation of Glu-57, the putative second general acid/base in catalysis, to an aspartic acid renders the final β-elimination step rate limiting.

Quorum sensing controls bacterial gene expression in response to cell density and is mediated by the production and detection of small signaling molecules called autoinducers (AIs)[1] (*1*). There are two types of AIs. The type 1 AI (AI-1) is species-specific; each bacterial species uses a unique AI-1 structure (e.g., acylhomoserine lactone) or a unique combination of AI-1s for intraspecies communication. The newly discovered type 2 AI (AI-2) is shared by many bacteria and is believed to function as a universal signal in interspecies communications (*2*, *3*). AI-2 is biosynthesized from *S*-adenosylhomocysteine (SAH), which is itself a byproduct of many *S*-adenosylmethionine-dependent methyltransferase reactions (Figure 1). SAH is hydrolyzed by a nucleosidase Pfs to adenine and *S*-ribosylhomocysteine (SRH). Subsequently, *S*-ribosylhomocysteinase (LuxS) converts SRH to homocysteine (Hcys) and 4,5-dihydroxy-2,3-pentanedione (DPD) (*4*−*6*). DPD spontaneously cyclizes to form a furanone, which is then complexed with borate to produce a furanosylborate diester as AI-2 (*7*).

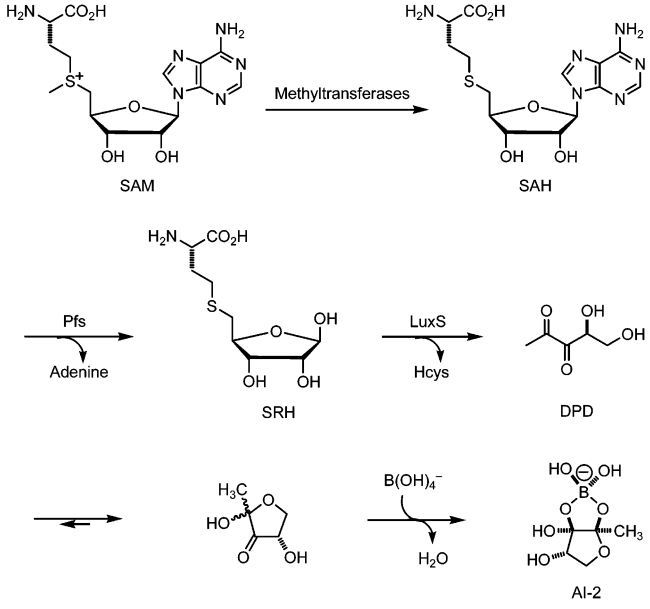

FIGURE 1: Biosynthetic pathway of AI-2.

LuxS is a mechanistically fascinating enzyme, which catalyzes formally the nonredox cleavage of a stable thioether bond. The mechanistic study of LuxS has been greatly facilitated by the availability of several high-resolution X-ray crystal structures of LuxS from *Bacillus subtilis*, *Helicobacter pylori*, *Haemophilus influenzae*, and *Deinococcus radiodurans*, both in their free forms and with bound SRH or Hcys (*8*−*10*). These studies revealed that LuxS from diverse species have the same overall fold and a highly conserved active site. LuxS exists as a homodimer and two identical

[†] This work was supported by grants from the National Institutes of Health (GM62820 and AI40575).

[‡] This paper is dedicated to Professor Christopher T. Walsh on the occasion of his 60th birthday.

* To whom correspondence should be addressed: Department of Chemistry, The Ohio State University, 100 West 18th Avenue, Columbus, OH 43210. Phone: (614) 688-4068; Fax: (614) 292-1532; E-mail: pei.3@osu.edu.

[1] Abbreviations: AI, autoinducer; SAH, *S*-adenosylhomocysteine; SRH, *S*-ribosylhomocysteine; Hcys, homocysteine; DPD, 4,5-dihydroxy-2,3-pentanedione; DTT, 1,4-dithio-DL-threitol; SAHH, *S*-adenosylhomocysteine hydrolase; DTNB, 5,5′-dithio-bis-(2-nitrobenzoic acid); KIE, kinetic isotope effect.

10.1021/bi0491088 CCC: $27.50
Published on Web 07/16/2004

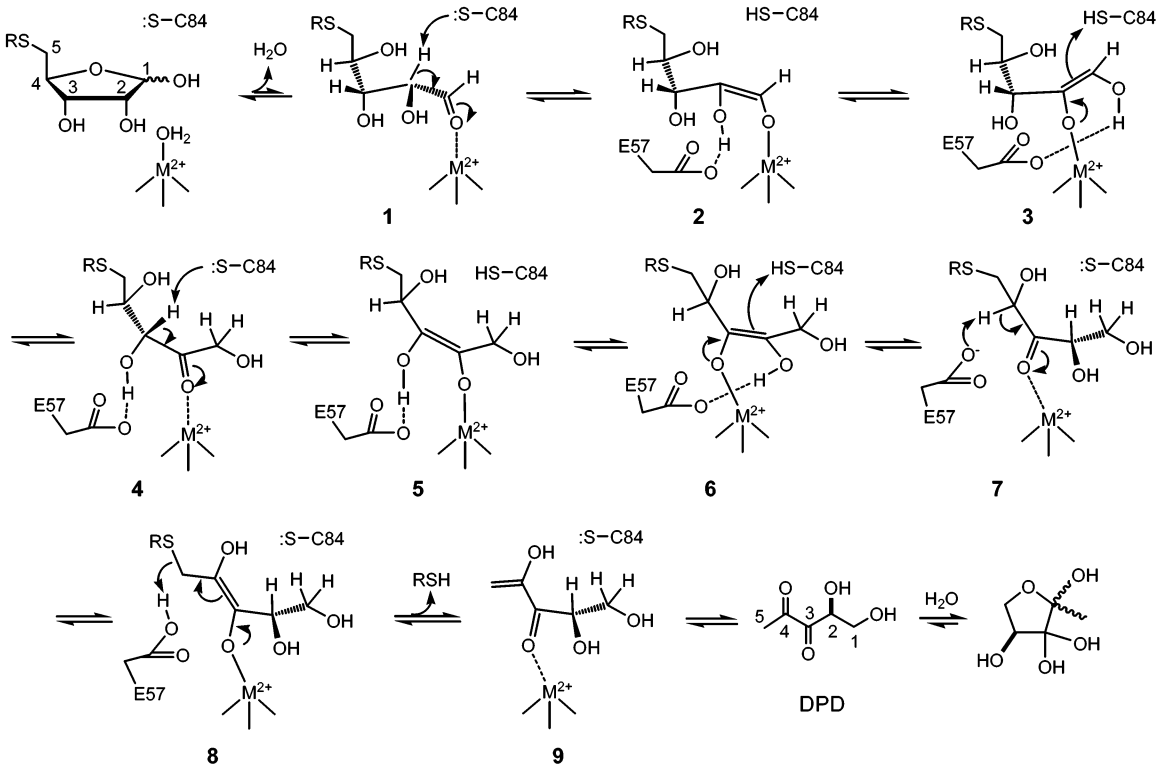

FIGURE 2: Proposed catalytic mechanism of LuxS. RSH, L-homocysteine.

active sites are formed at the dimer interface. Each active site contains a divalent metal ion, which was originally reported as a Zn^{2+} ion (*8*−*10*). We have recently showed that the native metal in LuxS is actually an Fe^{2+} ion, although substitution by other divalent metals such as Co^{2+} has minimal effect on LuxS activity (*11*). The metal ion is tetrahedrally coordinated by three conserved residues [His-54, His-58, and Cys-126 in *B. subtilis* LuxS (BsLuxS)] and a water molecule. On the basis of the X-ray crystal structures and the initial studies that have been conducted in this laboratory, we have recently proposed a catalytic mechanism for the LuxS-catalyzed reaction (Figure 2) (*11*, *12*). In an aqueous solution, SRH exists as the equilibrium between the open-chain, free aldehyde form and the ribose (hemiacetal) form. It is conceivable that LuxS may bind the ribose form and catalyze its ring opening. In the E·S complex **1**, the aldehyde carbonyl binds to the metal ion, displacing a bound water/hydroxide in the free enzyme. Coordination to the metal increases the acidity of the C2 proton, which is abstracted by a general base in the active site (likely Cys-84 in BsLuxS). The enediolate **2** formed undergoes ligand exchange, shifting the metal from C1 to the C2 OH group, presumably assisted by a second base/acid (likely Glu-57) and via a five-membered-ring transition state, to give enediolate **3**. Reprotonation at C1 position by Cys-84 and tautomerism back to the keto form generate a 2-keto intermediate **4**. Repetition of the above sequence shifts the carbonyl group to the C3 position to give a 3-keto intermediate **7**. Subsequent β-elimination, probably catalyzed by Glu-57 (or possibly a third acid/base), results in the release of Hcys as a free thiol and the formation of DPD in its enol form **9**. Enol **9** spontaneously tautomerizes to the keto form, either on its way of or after leaving the active site.

Substantial experimental evidence has been obtained for the above mechanism. When LuxS reaction was carried out in D_2O, deuterium was incorporated into the C1, C2, and C5 positions of DPD (*11*). The ketone intermediates have been observed in real time by ^{13}C NMR spectroscopy (*12*). Further, the 2-keto intermediate was chemically synthesized and demonstrated to be a chemically and kinetically competent intermediate on the catalytic pathway (*12*). However, although the deuterium exchange experiments have unambiguously established the involvement of proton transfers, the details of the transfer reactions (e.g., stereochemistry and the fate of protons) have not been resolved. In this work, we performed LuxS reactions with specifically deuterium-labeled SRH substrates and characterized the DPD derivatives by ^1H NMR spectroscopy and mass spectrometry. These experiments revealed both the regiochemistry and stereochemical course of the proton-transfer reactions. In addition, kinetic isotope effect was examined by LuxS activity assay and mass spectrometry.

EXPERIMENTAL PROCEDURES

Materials. [1′-^{2}H]Adenosine was purchased from Omicron Biochemicals, Inc. (South Bend, IN). L-4,4′-Dithio-bis(2-aminobutanoic acid) was purchased from Bachem (King of Prussia, PA). 1,4-Dithio-DL-threitol (DTT) solution was from New England Biolabs (Beverly, MA). D_2O (99.9% enrichment) was from Cambridge Isotope Laboratories (Andover, MA). All other chemicals and reagents were purchased from Sigma-Aldrich. *S*-Adenosylhomocysteine hydrolase (SAHH), nucleosidase Pfs, and wild-type and mutant Co(II)-substituted LuxS were overexpressed in *Escherichia coli* and purified to near homogeneity as previously described (*11*, *12*).

Synthesis of [2′-^{2}H]adenosine and [3′-^{2}H]adenosine. [2′-^{2}H]adenosine and [3′-^{2}H]adenosine were chemically synthesized using the procedure of Frey (*13*) with the following modification. After reduction with $NaBD_4$, the

tritylated [2′-^{2}H]adenosine and [3′-^{2}H]adenosine were deprotected by following the method of MacCoss and Cameron (*14*).

Preparation of [1′-^{2}H], [2′-^{2}H], [3′-^{2}H], and [4′-^{2}H]SAH. L-4,4′-Dithio-bis(2-aminobutanoic acid) was reduced with one equivalent of DTT at pH 12 for 3.5 h. The crude Hcys (10 mM) was added to [1′-^{2}H], [2′-^{2}H] or [3′-^{2}H]adenosine (10 mM) in a buffer containing 50 mM $NaH_2PO_4-Na_2HPO_4$ (pH 7.0) and 50 mM NaCl, followed by the addition of SAHH (final 5 μM). After overnight incubation at room temperature, the reaction mixture was purified by reversed-phase HPLC on a semipreparative C18 column (Vydac). The column was eluted with a 30-min linear gradient of 10−100% acetonitrile in water (monitored at 260 nm). SAH eluted at ∼7 min. [1′-^{2}H]SAH: ^{1}H NMR (400 MHz, D_2O): δ 8.27 (s, 1H, aromatic), 8.18 (s, 1H, aromatic), 5.98 (d, 0.08H, C1′−H, J = 5.2 Hz), 4.76 (d, 1H, C2′−H, J = 5.4 Hz), 4.32 (dd, 1H, C3′−H, J = 4.4, 5.2 Hz), 4.23 (m, 1H, C4′−H), 3.71 (dd, 1H, αH, J = 5.4, 7.2 Hz), 2.96 (dd, 1H, C5′−H, J = 5.0, 14.2 Hz), 2.88 (dd, 1H, C5′−H, J = 6.7, 14.2 Hz), 2.58 (dd, 2H, γH, J = 7.5, 7.6 Hz), 2.09 ∼ 1.92 (m, 2H, βH). ESI-MS: $C_{14}H_{19}DO_5N_6SH^+$ ([M + H]$^+$) calcd 386.1328, found 385.14 (7.5%), 386.15 (100%). [3′-^{2}H]SAH: ^{1}H NMR (250 MHz, D_2O): δ 8.44 (s, 1H, aromatic), 8.36 (s, 1H, aromatic), 6.06 (d, 1H, C1′−H, J = 4.8 Hz), 4.78 (d, 1H, C2′−H, J = 4.8 Hz), 4.26 (dd, 1H, C4′−H, J = 4.6, 5.3 Hz), 3.85 (dd, 1H, αH, J = 5.4, 7.4 Hz), 3.00 (dd, 1H, C5′−H, J = 5.0, 14.1 Hz), 2.91 (dd, 1H, C5′−H, J = 5.4, 14.1 Hz), 2.65 (dd, 2H, γH, J = 7.4, 7.5 Hz), 2.18 ∼ 1.96 (m, 2H, βH). HRESI-MS: $C_{14}H_{19}DO_5N_6SNa^+$ ([M + Na]$^+$) calcd 408.1170, found 408.1168. [4′-^{2}H]SAH was prepared from adenosine as described above except that a D_2O buffer (50 mM $NaH_2PO_4-Na_2HPO_4$, pD 7.0, 50 mM NaCl) was used in all steps (*15*). Prior to use, SAHH was exchanged into the D_2O buffer in an Amicon concentrator (Millipore). ^{1}H NMR (250 MHz, D_2O): δ 8.43 (s, 1H, aromatic), 8.36 (s, 1H, aromatic), 6.06 (d, 1H, C1′−H, J = 5.0 Hz), 4.80 (dd, 1H, C2′−H, J = 5.2, 5.3 Hz), 4.36 (d, 1H, C3′−H, J = 5.1 Hz), 3.82 (dd, 1H, αH, J = 5.2, 7.5 Hz), 3.00 (d, 1H, C5′−H, J = 14.3 Hz), 2.92 (d, 1H, C5′−H, J = 14.1 Hz), 2.63 (dd, 2H, γH, J = 7.2, 8.0 Hz), 2.15 ∼ 1.93 (m, 2H, βH). HRESI-MS: $C_{14}H_{19}DO_5N_6SNa^+$ ([M + Na]$^+$) calcd 408.1170, found 408.1168. [2′-^{2}H]SAH was still contaminated with some unknown species after HPLC; its spectral data were not obtained.

Preparation of [1-^{2}H], [2-^{2}H], [3-^{2}H], and [4-^{2}H]SRH. Pfs (5 μM) was added to the properly labeled SAH from above (10 mM) and the reaction was incubated overnight. The resulting SRH was used directly in LuxS reactions without further treatment. The concentration of SRH was determined by mixing SRH and Co(II)-LuxS, allowing the reaction to go to completion, and assaying the amount of Hcys formed using 5,5′-dithio-bis-(2-nitrobenzoic acid) (DTNB) (*16*).

*Characterization of LuxS Products **10**−**13**.* Properly deuterated SRH (1.0 mM), Co(II)-LuxS of *B. subtilis* (1.0 mg/mL), and 1,2-phenylenediamine (1.0 mM) were mixed in a buffer containing 50 mM $NaH_2PO_4-Na_2HPO_4$ (pH 7.0) and 50 mM NaCl (total reaction volume = 1 mL) and incubated at room temperature for 20 h. Under these conditions, the conversion of SRH to DPD and homocysteine was essentially complete. At this point, additional 1,2-phenylenediamine was added to make a final concentration of 2 mM and the pH of the reaction mixture was adjusted to 4.5 by the addition of 2 M HCl. The resulting solution was incubated for another 20 h. The reaction mixture was extracted with ethyl acetate (4 × 0.4 mL) and the organic layer was concentrated to ∼100 μL under reduced pressure. The crude product was purified by reversed-phase HPLC on a C18 column (Vydac). The column was eluted with a 30-min linear gradient of 10−100% acetonitrile in water (monitored at 240 nm). The desired quinoxaline product eluted at ∼40% acetonitrile. Quinoxaline **10** (from [1-^{2}H]SRH): ^{1}H NMR (400 MHz, $CDCl_3$): δ 8.06 ∼ 8.01 (m, 2H, aromatic), 7.78 ∼ 7.72 (m, 2H, aromatic), 5.11 (d, 1H, C2−H, J = 3.4 Hz), 4.01 (d, 1H, C1−H, J = 3.3 Hz), 3.84 (dd, 0.15H, C1−H, J = 5.5, 11.5 Hz), 2.81 (s, 3H, CH_3). ESI-MS: $C_{11}H_{11}DO_2N_2H^+$ ([M + H]$^+$) calcd 206.1016, found 205.11 (5.8%), 206.12 (44%). Quinoxaline **11** (from [2-^{2}H]SRH): ^{1}H NMR (400 MHz, $CDCl_3$): δ 8.08−8.05 (m, 2H, aromatic), 7.78−7.75 (m, 2H, aromatic), 5.12 (dd, 1H, C2−H, J = 3.6, 5.4 Hz), 4.04 (dd, 0.6H, C1−H, J = 3.4, 11.7 Hz), 3.84 (dd, 1H, C1−H, J = 5.5, 11.7 Hz), 2.86 (s, 3H, CH_3). HRESI-MS: $C_{11}H_{11}DO_2N_2Na^+$ ([M + Na]$^+$) calcd 228.0853, found 228.0848 (5%). Quinoxaline **12** (from [3-^{2}H]SRH): ^{1}H NMR (400 MHz, $CDCl_3$): δ 8.06−8.02 (m, 2H, aromatic), 7.76−7.72 (m, 2H, aromatic), 5.12 (b, 0.1H, C2−H), 4.03 (d, 1H, C1−H, J = 11.6 Hz), 3.84 (d, 1H, C1−H, J = 11.6 Hz), 2.81 (s, 3H, CH_3). HRESI-MS: $C_{11}H_{11}DO_2N_2Na^+$ ([M + Na]$^+$) calcd 228.0853, found 227.0778 (10%), 228.0834 (100%). Quinoxaline **13** (from [4-^{2}H]SRH): ^{1}H NMR (250 MHz, $CDCl_3$): δ 8.07−8.01 (m, 2H, aromatic), 7.78−7.71 (m, 2H, aromatic), 5.12 (dd, 1H, C2−H, J = 3.5, 5.4 Hz), 4.04 (dd, 1H, C1−H, J = 3.5, 11.5 Hz), 3.84 (dd, 1H, C1−H, J = 5.6, 11.5 Hz), 2.81 (s, 3H, CH_3). HRESI-MS: $C_{11}H_{12}O_2N_2Na^+$ ([M + Na]$^+$) calcd 227.0791, found 227.0789.

*Stereochemistry of LuxS Products **14**−**16**.* The purified quinoxaline derivatives from above (compounds **10**, **11**, and **13**) were each dissolved in anhydrous CH_2Cl_2 and mixed with six equivalents of pyridine. Two equivalents of phosgene (20% solution in toluene) were added and the reaction was allowed to proceed in an ice-water bath and under argon for 1 h. The reaction mixture was extracted with 5% HCl and water, and the organic layer was evaporated to give carbonate diesters **14**−**16**, respectively. Derivative **14**: ^{1}H NMR (250 MHz, $CDCl_3$): δ 8.08−8.03 (m, 2H, aromatic), 7.78−7.72 (m, 2H, aromatic), 6.01 (dd, 1H, C2−H, J = 6.6, 8.2 Hz), 5.54 (dd, 1H, C1−H, J = 6.6, 8.5 Hz), 4.76 (dd, 1H, C1−H, J = 8.3, 8.4 Hz), 2.84 (s, 3H, CH_3). HRESI-MS: $C_{12}H_{10}O_3N_2H^+$ ([M + H]$^+$) calcd 231.0764, found 231.0774. Derivative **15**: ^{1}H NMR (250 MHz, $CDCl_3$): δ 8.08−8.03 (m, 2H, aromatic), 7.80−7.71 (m, 2H, aromatic), 6.06 (d, 1H, C2−H, J = 8.1 Hz), 5.60 (dd, 0.15H, C1−H, J = 6.5, 8.5 Hz), 4.82 (d, 1H, C1−H, J = 8.1 Hz), 2.87 (s, 3H, CH_3). Derivative **16**: ^{1}H NMR (400 MHz, $CDCl_3$): δ 8.08−8.04 (m, 2H, aromatic), 7.80−7.73 (m, 2H, aromatic), 6.05 (dd, 1H, C2−H, J = 6.6, 8.1 Hz), 5.59 (dd, 1H, C1−H, J = 6.6, 8.5 Hz), 4.81 (dd, 0.6H, C1−H, J = 8.3, 8.4 Hz), 2.90 (s, 3H, CH_3).

LuxS Activity Assay. LuxS reaction (total volume = 200 μL) was performed in a buffer containing 50 mM HEPES (pH 7.0), 150 mM NaCl, and 150 μM DTNB. The concentration of deuterated SRH varied from 0 to 34 μM for *B. subtilis* LuxS and up to 180 μM for *V. harveyi* LuxS. The

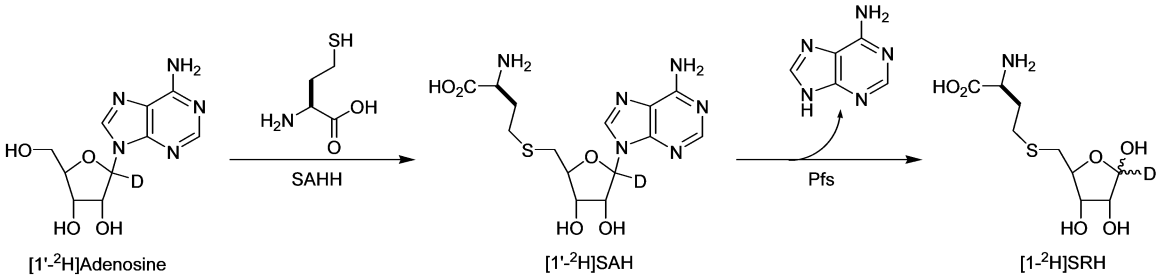

FIGURE 3: Enzymatic synthesis of deuterium-labeled substrate, [1-^{2}H]SRH.

reaction was initiated by the addition of Co(II)-LuxS (final concentration 0.4 μM) and monitored continuously at 412 nm in a Perkin-Elmer λ25 UV−vis spectrophotometer at room temperature. The initial rates obtained from the early regions of the progress curves (~3 min for *B. subtilis* LuxS and ~30 s for *V. harveyi* LuxS) were fitted into the Michaelis−Menten equation using KaleidaGraph 3.6.

Deuterium Kinetic Isotope Effect. Approximately equimolar concentrations of unlabeled SRH and [1-^{2}H], [2-^{2}H] or [3-^{2}H]SRH (~1.5 mM each) were mixed in a buffer containing 50 mM NaH_2PO_4−Na_2HPO_4 (pH 7.0) and 50 mM NaCl (total reaction volume = 0.6 mL). The reaction was initiated by the addition of *B. subtilis* Co(II)-LuxS (1 mg/mL), allowed to reach ≤10% completion (~20 min), and quenched with the addition of 3 volumes of methanol. After evaporation of the methanol under reduced pressure, 1,2-phenylenediamine (final 1.5 mM) was added to the solution and the pH was adjusted to 4.5. The reaction mixture was incubated overnight at room temperature and extracted with ethyl acetate (4 × 0.4 mL). The organic layer was collected and analyzed by LC-T electrospray ionization mass spectrometry. For the reaction involving [4-^{2}H]SRH, a ~1:1 mixture of [3-^{13}C]SRH (*12*) and [4-^{2}H]SRH was employed and analyzed in the same fashion. The reactions using *V. harveyi* Co(II)-LuxS E57D (1.5 mg/mL, for 45 min) were carried out as described above.

RESULTS AND DISCUSSION

Chemo-Enzymatic Synthesis of Deuterium-Labeled SRH. This was accomplished by taking advantage of the fact that the reaction catalyzed by SAHH is reversible and the equilibrium lies far in the direction of SAH synthesis (*17*). Thus, [1′-^{2}H]SAH was prepared by overnight incubation of [1′-^{2}H]adenosine, Hcys, and SAHH at pH 7. Subsequent treatment with Pfs converted [1′-^{2}H]SAH to [1-^{2}H]SRH (Figure 3). [2-^{2}H]SRH and [3-^{2}H]SRH were similarly synthesized from the corresponding deuterated adenosines, which were chemically synthesized using a procedure previously described by Frey and co-workers (*13*). [4-^{2}H]-SRH was prepared by incubating unlabeled adenosine, Hcys, and SAHH in a D_2O buffer followed by treatment with Pfs (*15*).

Regiochemistry of Proton Transfer. According to the proposed LuxS mechanism, an active site base (Cys-84 in BsLuxS) abstracts the proton at ribose C2 position and later adds it back to the C1 position (Figure 2). Similarly, the ribose C3 proton is migrated to the C2 position in DPD (to avoid confusion, the DPD carbon chain is so numbered that its carbon C1 is derived from the ribose C1 atom). On the other hand, the C1 proton should remain at the same position in DPD, whereas the C4 proton would be lost to solvent upon β-elimination of the 3-keto intermediate (Figure 2). To test the validity of this hypothesis, we carried out the LuxS reaction with SRH specifically deuterated at C1−4 positions and analyzed the reaction products by ^{1}H NMR spectroscopy and mass spectrometry. Unless stated otherwise, all of the experiments in this work employed the Co(II)-substituted BsLuxS, which has essentially the same catalytic properties as the native LuxS (Fe^{2+} form) but is much more stable than the latter (*11*). Due to difficulty in directly isolating DPD, the reaction product formed was converted into the corresponding quinoxaline derivative by treatment with 1,2-phenylenediamine in situ and isolated by HPLC (*11*). The quinoxaline derivative derived from [2-^{2}H]SRH (Compound **11**) showed three double-doublets in the δ 3.8−5.1 region of its ^{1}H NMR spectrum, corresponding to the three C1 and C2 protons (Figures 4a and 5a). The resonance at δ 4.0, which had previously been assigned to one of the C1 protons (*11*), only has an intensity of 0.6 H. Mass-spectrometric analysis revealed the presence of a deuterated product at *m*/*z* 228.0848 (calculated molecular mass for $C_{11}H_{11}DO_2N_2$-Na^+ = 228.0853). In addition, the signals for the other C1 proton (δ 3.8) and the C2 proton (δ 5.1) are noticeably broadened. These results indicate that compound **11** is a 6:4 mixture of two species; the major species has a proton at the C1 position, whereas the minor species has a deuterium. Thus, 40% of the deuterium at the C2 position of SRH was transferred to C1 as a result of the LuxS reaction, providing direct proof for the proposed proton transfer mechanism (Figures 2 and 5a). The 0.6 H at product C1 position is due to proton exchange with solvent, which had previously been observed when the LuxS reaction was carried out in D_2O (*11*). When [3-^{2}H]SRH was used as substrate, the ^{1}H NMR of the product (compound **12**) showed two broadened doublets at δ 4.0 and δ 3.8, whereas the signal at δ 5.1 (C2 proton) had an intensity of only ~0.1 H (Figure 4b). The mass spectrum of compound **12** showed two peaks at *m*/*z* 227.0778 (10% intensity) and *m*/*z* 228.0834 (100% intensity). This indicates that the deuterium at C3 position of [3-^{2}H]-SRH was nearly quantitatively transferred to the C2 position of DPD product (Figure 5b). The broadened peaks are due to coupling between the C1 protons and the C2 deuterium.

To determine the fate of the C4 proton, the reaction was similarly carried out with [4-^{2}H]SRH. The ^{1}H NMR spectrum of the resulting quinoxaline derivative (**13**) was identical to that derived from the unlabeled SRH (*11*), with each of the three C1 and C2 protons producing a double-doublet (Figures 4c and 5c). Its mass spectrum showed a peak at *m*/*z* 227.0789 and the natural isotope peaks, but no evidence for a deuterated species (calculated *m*/*z* 228.0853). This indicates

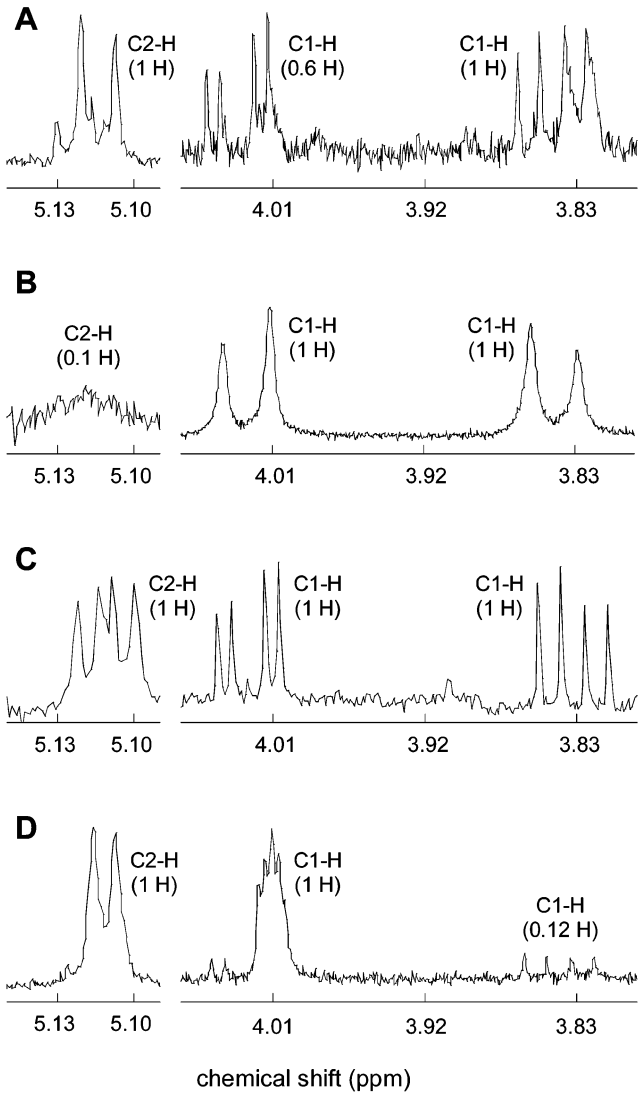

FIGURE 4: ^{1}H NMR spectra (400 MHz, $CDCl_3$) of quinoxaline derivatives obtained from various deuterated SRH: (A) from [2-^{2}H]-SRH (compound **11**), (B) from [3-^{2}H]SRH (compound **12**), (C) from [4-^{2}H]SRH (compound **13**), and (D) from [1-^{2}H]SRH (compound **10**).

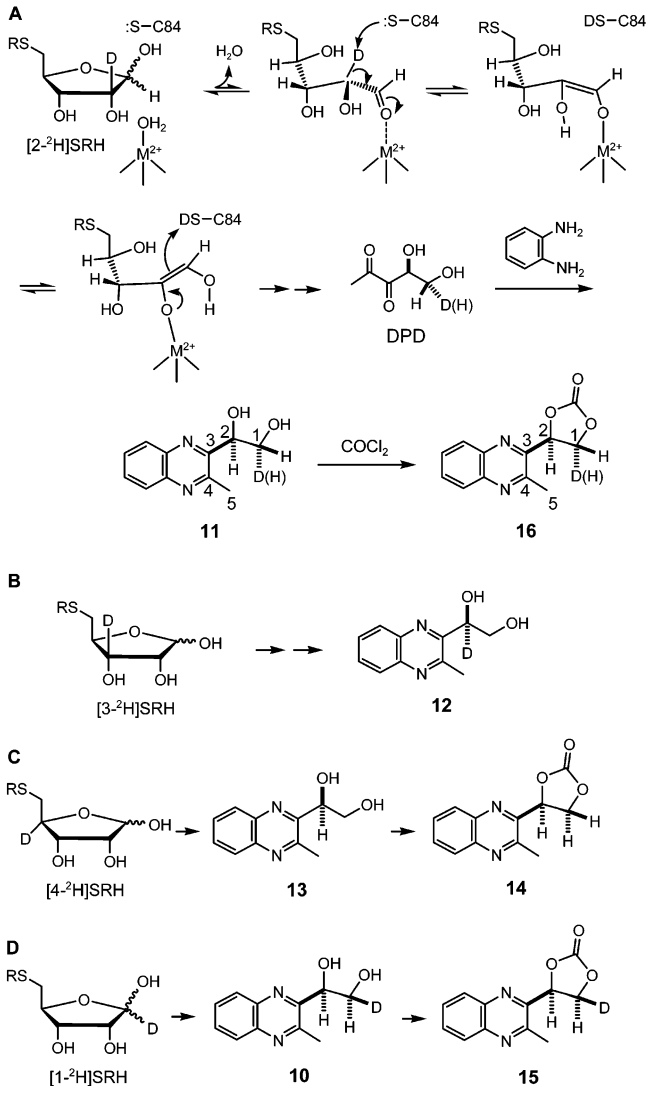

FIGURE 5: Structures and/or mechanism of formation of quinoxaline derivatives **10**−**13** and the cyclized carbonate diesters **14**−**16**.

that the C4 deuterium was completely lost to solvent upon β-elimination of the 3-keto intermediate (Figure 5c). For comparison, the reaction with [1-^{2}H]SRH was also performed. The C2 proton showed a doublet at δ 5.1, whereas the C1 proton produced a multiplet at δ 4.0 (Figure 4d). Surprisingly, a small but detectable peak appeared at δ 3.8 (~0.12 H), which was also evident from its mass spectrum as a peak at *m*/*z* 205.11 (not shown). Mass spectrometric analysis of [1′-^{2}H]SAH revealed that part of the proton signal in the quinoxaline product (**10**) came from incomplete deuteration of the substrate (93%). Control experiments had previously shown that no H/D exchange occurs during the conversion of DPD into the quinoxaline derivatives (*11*). These results indicate that there was a small amount (~5%) of proton exchange at the C1 position during the LuxS reaction. We tentatively attribute this to proton exchange at the 2-keto intermediate stage, which could take place via either or both of the following mechanisms. First, the 2-keto intermediate, which is at least partially released from the enzyme active site (*12*), can undergo nonenzymatic proton exchange at the C1 position before being rebound by the enzyme and converted into the product. Second, the enzyme-catalyzed reverse reaction, from 2-keto intermediate **4** back to SRH, may not be completely stereospecific (Figure 2); removal of the C1 deuterium instead of the proton would result in loss of the C1 label. We have previously demonstrated that in the presence of LuxS, SRH and the 2-keto intermediate are rapidly interconverted (*12*).

Stereochemical Course of Proton Transfer. Quinoxaline derivatives **10** and **11**, derived from [1-^{2}H]SRH and [2-^{2}H]-SRH, respectively, gave different ^{1}H NMR spectra (compare Figures 4a and 4d), although both contain a deuterium at C1 position. For **11**, the proton at δ 4.0 is partially replaced by deuterium, whereas deuterium substituted the proton at δ 3.8 in quinoxaline **10**. This suggests that the proton-transfer reactions are stereospecific (at least in the forward direction). The proposed mechanism predicts that the same general acid/base (Cys-84) catalyzes the proton-transfer reactions leading to the formation of 2-keto and 3-keto intermediates and that proton abstraction and addition all occur at the same face of the enediolate intermediate (Figure 2). To test this hypothesis, the quinoxaline derivatives **10**, **11**, and **13** were converted into cyclic carbonate diesters **15**, **16**, and **14**, respectively (Figure 5). Cyclization reduces the conformational flexibility of the molecule, thus facilitating conformational analysis by

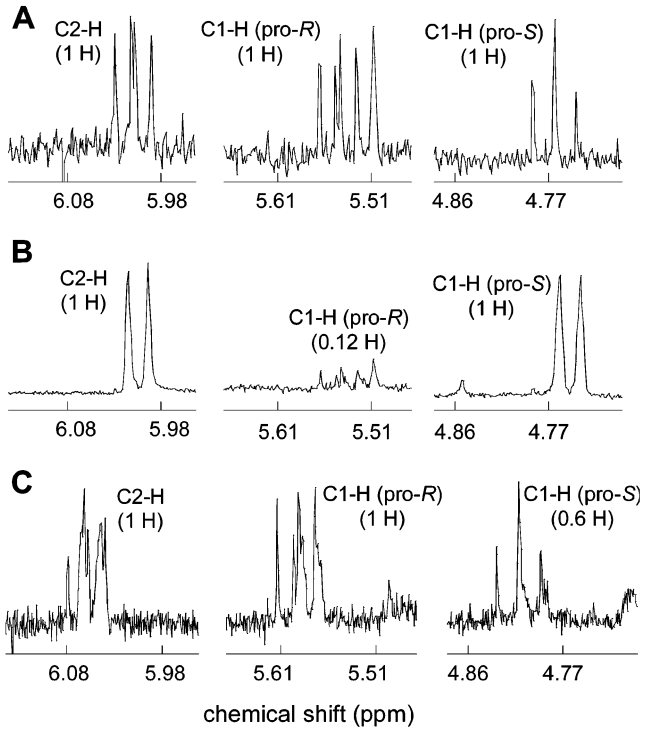

FIGURE 6: ^{1}H NMR spectra (400 MHz, $CDCl_3$) of cyclic carbonate diesters **14**−**16**.

NMR spectroscopy. The ^{1}H NMR spectrum of the unlabeled quinoxaline diester (**14**) has three double doublets at δ 6.0, 5.5 and 4.8, which were assigned to the C2, C1 pro-*R*, and C1 pro-*S* protons, respectively (Figure 6a). The ^3J coupling constant between C2 and C1 pro-*S* protons, which are in cis configuration with respect to the five-membered ring, is 8.2 Hz, whereas the coupling constant between C2 and C1 pro-*R* protons (trans) is 6.6 Hz. The ^2J value between the two C1 protons is 8.4 Hz. The quinoxaline diester **15**, which is derived from [1-^{2}H]SRH, has a reduced signal at δ 5.6 and a coupling constant of 8.1 Hz between the signals at δ 6.1 and 4.8 (Figure 6b). The large ^3J value is consistent with a cis configuration for the two vicinal protons (Figure 5d). The diester **16** derived from [2-^{2}H]SRH has a weaker signal (0.6 H) at δ 4.8 and *J* values of 8.3 and 8.4 Hz. The coupling constant between the δ 6.1 and 5.6 protons is 6.6 Hz (Figure 6c), indicating a trans configuration between the C2 proton and the unexchanged C1 proton (Figure 5a). Since the absolute stereochemistry at the C2 position of DPD has previously been established as having an *S* configuration through X-ray crystallography (*7*), compound **15** must have an *S* configuration at its C1 position (Figure 5d). Likewise, the C1 in compound **16** must have an *R* configuration (Figure 5a). Therefore, our results are consistent with the mechanistic proposal that the proton abstraction and addition all take place at the same face of the enediolate intermediates (suprafacial proton transfer). It provides further evidence for the involvement of a single monoprotic base (Cys-84) in the early proton-transfer steps (up to the formation of the 3-keto intermediate).

Deuterium Kinetic Isotope Effect. The primary kinetic isotope effect was first examined by comparing the overall reaction rates using unlabeled as well as the various deuterated SRH as substrates. No significant kinetic isotope effect was observed for [1-^{2}H], [2-^{2}H], or [4-^{2}H]SRH with either *B. subtilis* or *V. harveyi* LuxS (Table 1). However, a small kinetic isotope effect ($k_H/k_D = 1.3-1.4$) was observed for [3-^{2}H]SRH (Table 1). This indicates that abstraction of the C3 proton or addition of this proton back to the C2 carbon is partially rate limiting on the catalytic pathway, whereas the other proton-transfer steps are quite rapid. NMR studies with ^{13}C-labeled SRH have previously shown that conversion of the 2-keto intermediate (**4**) to the 3-keto intermediate (**7**) is at least partially rate limiting (*12*). However, quantitative interpretation of the overall kinetic isotope effect is complicated, due to release of the keto intermediates from the active site during catalysis (*12*). The magnitude of the kinetic isotope effect can be suppressed by committing more enzyme to the rate-limiting step.

To obtain a more reliable measure of kinetic isotope effect, the LuxS reaction was performed in a solution containing an approximately 1:1 ratio of SRH and deuterated SRH, with the unlabeled SRH serving as an internal standard. The reaction time was controlled so that ≤10% of the SRH was converted to DPD. After the reaction was quenched, the reaction products were derivatized with 1,2-phenylenediamine and subjected to mass spectrometric analysis. The KIE value was calculated from the ratio of unlabeled and labeled products. For the reaction with SRH/[1-^{2}H]SRH, two molecular ion peaks at *m*/*z* 205 ($[M + H]^+$) and 206 ($[M + D]^+$) were observed, with an intensity ratio of 1.35:1. After taking into account the 12% deuterium loss due to incomplete deuteration and solvent exchange (see above), the products from SRH and [1-^{2}H]SRH yielded a KIE of 1.1:1, in good agreement with the result from direct LuxS activity assay (Table 1). The reaction with SRH/[2-^{2}H]SRH or SRH/[3-^{2}H]SRH resulted in two products with *m*/*z* 227 ($[M + Na]^+$) and 228 ($[M + D - H + Na]^+$) and k_H/k_D ratios of 1.1:1 and 1.7:1, respectively (after correction for loss of deuterium to solvent), again in good agreement with the values obtained from direct assays (Table 1). To examine the kinetic isotope effect of the final β-elimination reaction, a mixture of [3-^{13}C]SRH (*12*) and [4-^{2}H]SRH was used since both SRH and [4-^{2}H]SRH would give the same product. The reaction resulted in two products with *m*/*z* 227 ($[M + Na]^+$) and 228 ($[M + {}^{13}C + Na]^+$) and a k_H/k_D ratio of 1:1.1. Next, a catalytically impaired LuxS mutant, in which the second general acid/base critical for the β-elimination reaction

Table 1: LuxS Activity toward SRH and Deuterated SRH

	Co-LuxS (Bs)				Co-Lux S (Vh)			
substrate	k_{cat} (s^{-1})	K_M (μM)	k_{cat}/K_M (M^{-1} s^{-1})	k_H/k_D	k_{cat} (s^{-1})	K_M (μM)	k_{cat}/K_M (M^{-1} s^{-1})	k_H/k_D
SRH	0.029 ± 0.001	2.2 ± 0.5	1.3×10^4		0.40 ± 0.01	39 ± 1	1.0×10^4	
[1-^{2}H]SR H	0.030 ± 0.002	2.1 ± 0.2	1.4×10^4	1.0	0.42 ± 0.01	40 ± 2	1.0×10^4	1.0
[2-^{2}H]SR H	0.029 ± 0.002	2.3 ± 0.2	1.3×10^4	1.0	0.36 ± 0.04	38 ± 6	0.9×10^4	1.1
[3-^{2}H]SR H	0.023 ± 0.001	2.2 ± 0.1	1.0×10^4	1.3	0.28 ± 0.03	39 ± 4	0.7×10^4	1.4
[4-^{2}H]SR H	0.029 ± 0.002	2.0 ± 0.5	1.4×10^4	1.0	0.39 ± 0.01	39 ± 2	1.0×10^4	1.0

(Glu-57) is replaced by aspartic acid, was employed in the above experiments. When SRH/[1-^{2}H]SRH were used as substrates, a k_H/k_D ratio of 1.1:1 was obtained, whereas the ratio was 4.6:1 when [3-^{13}C]SRH/[4-^{2}H]SRH were substrates. Taken together, the above results demonstrate that for wild-type LuxS, the proton transfer steps are generally very rapid events; they become only partially rate-limiting during the conversion of 2-keto intermediate **4** to 3-keto intermediate **7**. Therefore, other steps such as metal−ligand exchange and/or protein conformational change(s) must be rate limiting in WT LuxS. However, mutation of the catalytic bases can slow the proton-transfer steps and render them rate limiting. This significant kinetic isotope effect observed for E57D LuxS-catalyzed cleavage of [4-^{2}H]SRH suggests that Glu-57 is the general base that abstracts the C4 proton during the β-elimination reaction. It has previously been reported that mutation of Glu-57 to alanine resulted in substantially increased accumulation of intermediate **7** (*12*).

CONCLUSION

We have elucidated both the regiochemistry and the stereochemistry of the proton transfer steps in the LuxS-catalyzed reaction. These results suggest that two monoprotic acids/bases, Cys-84 and Glu-57, are most likely responsible for catalyzing all of the proton transfer reactions. KIE studies indicate that the proton transfer steps are generally quite rapid, with the exception of conversion of the 2-keto intermediate to 3-keto intermediate, where proton transfer is partially rate limiting. All of these results are consistent with the previously proposed LuxS mechanism (*11*, *12*).

REFERENCES

1. Miller, M. B. and Bassler, B. L. (2001) Quorum sensing in bacteria, *Annu. Rev. Microbiol. 55*, 165−199.
2. Federle, M. J. and Bassler, B. L. (2003) Interspecies communication in bacteria, *J. Clin. Invest. 112*, 1291−1299.
3. Xavier, K. B. and Bassler, B. L. (2003) LuxS quorum sensing: more than just a numbers game, *Curr. Opin. Microbiol. 6*, 191−197.
4. Miller, C. H. and Duerre, J. A. (1968) *S*-Ribosylhomocysteine cleavage enzyme from *Escherichia coli*, *J. Biol. Chem. 243*, 92−97.
5. Surette, M. G., Miller, M. B., and Bassler, B. L. (1999) Quorum sensing in *Escherichia coli*, Salmonella *typhimurium*, and *Vibrio harveyi*: a new family of genes responsible for autoinducer production, *Proc. Natl. Acad. Sci. U.S.A. 96*, 1639−1644.
6. Schauder, S., Shokat, K., Surette, M. G., and Bassler, B. L. (2001) The LuxS family of bacterial autoinducers: biosynthesis of a novel quorum-sensing signal molecule, *Mol. Microbiol. 41*, 463−476.
7. Chen, X., Schauder, S., Potier, N., van Dorsselaer, A., Pelczer, I., Bassler, B. L., and Hughson, F. M. (2002) Structural identification of a bacterial quorum-sensing signal containing boron, *Nature 415*, 545−549.
8. Lewis, H. A., Furlong, E. B., Laubert, B., Eroshkina, G. A., Batiyenko, Y., Adams, J. M., Bergseid, M. G., Marsh, C. D., Peat, T. S., Sanderson, W. E., Sauder, J. M., and Buchanan, S. G. (2001) A structural genomics approach to the study of quorum sensing: crystal structures of three LuxS orthologs, *Structure 9*, 527−537.
9. Hilgers, M. T., and Ludwig, M. L. (2001) Crystal structure of the quorum-sensing protein LuxS reveals a catalytic metal site, *Proc. Natl. Acad. Sci. U.S.A. 98*, 11169−11174.
10. Ruzheinikov, S. N., Das, S. K., Sedelnikova, S. E., Hartley, A., Foster, S. J., Horsburgh, M. J., Cox, A. G., McCleod, C. W., Mekhalfia, A., Balckburn, G. M., Rice, D. W., and Baker, P. J. (2001) The 1.2 Å structure of a novel quorum-sensing protein, *Bacillus subtilis* LuxS, *J. Mol. Biol. 313*, 111−122.
11. Zhu, J., Dizin, E., Hu, X., Wavreille, A., Park, J., and Pei, D. (2003) *S*-Ribosylhomocysteinase (LuxS) is a mononuclear iron protein, *Biochemistry 42*, 4717−4726.
12. Zhu, J., Hu, X., Dizin, E., and Pei, D. (2003) Catalytic mechanism of *S*-ribosylhomocysteinase (LuxS): direct observation of ketone intermediates by ^{13}C NMR spectroscopy, *J. Am. Chem. Soc. 125*, 13379−13381.
13. Magnusson, O. Th., Reed, G. H., and Frey, P. A. (2001) Characterization of an allylic analogue of the 5′-deoxyadenosyl radical: an intermediate in the reaction of lysine 2,3-aminomutase, *Biochemistry 40*, 7773−7782.
14. MacCoss, M. and Cameron, D. J. (1978) Facile detritylation of nucleoside derivatives by using trifluoroacetic acid, *Carbohydr. Res. 60*, 206−209.
15. Palmer, J. and Abeles, R. (1979) The mechanism of action of *S*-adenosylhomocysteine, *J. Biol. Chem. 254*, 1217−1226.
16. Ellman, G. L. (1959) Tissue sulfhydryl groups, *Arch. Biochem. Biophys. 82*, 70−77.
17. Takata, Y., Yamada, T., Huang, Y., Komoto, J., Gomi, T., Ogawa, H., Fujioka, M., and Takusagawa, F. (2002) Catalytic mechanism of *S*-adenosylhomocysteine hydrolase: site-directed mutagenesis of Asp-130, Lys-185, Asp-189, and Asn-190, *J. Biol. Chem. 277*, 22670−22676.

BI0491088